Scientific Research Publishing

Journal of Power and Energy Engineering, 2024, 12, 60-74
https://www.scirp.org/journal/jpee
ISSN Online: 2327-5901
ISSN Print: 2327-588X

Optimization of the Gas Generator in Composite Power System with Tip-Jet Rotor

Jianxiang Tang[1], Yifei Wu[1]*, Yun Wang[2], Jinwu Wu[1]

[1]School of Aircraft Engineering, Nanchang Hangkong University, Nanchang, China
[2]School of Intelligent Manufacturing, Taizhou University, Taizhou, China
Email: *wuyifei@nchu.edu.cn

How to cite this paper: Tang, J.X., Wu, Y.F., Wang, Y. and Wu, J.W. (2024) Optimization of the Gas Generator in Composite Power System with Tip-Jet Rotor. *Journal of Power and Energy Engineering*, **12**, 60-74.
https://doi.org/10.4236/jpee.2024.123005

Received: February 28, 2024
Accepted: March 24, 2024
Published: March 27, 2024

Abstract

The key and bottleneck of research on the tip-jet rotor compound helicopter lies in the power system. Computational Fluid Dynamics (CFD) was used to numerically simulate the gas generator and rotor inner passage of the tip-jet rotor composite power system, studying the effects of intake mode, inner cavity structure, propellant components, and injection amount on the characteristics of the composite power system. The results show that when a single high-temperature exhaust gas enters, the gas generator outlet fluid is uneven and asymmetric; when two-way high-temperature exhaust gas enters, the outlet temperature of the gas generator with a tilted inlet is more uniform than that with a vertical inlet; adding an inner cavity improves the temperature and velocity distribution of the gas generator's internal flow field; increasing the energy of the propellant is beneficial for improving the available moment.

Keywords

Tip-Jet Driven Rotor, Composite Power System, Gas Generator Optimization, Hydrogen Peroxide, Aerodynamic Characteristics, Numerical Simulation

1. Introduction

Modern helicopters are evolving towards high speed, high efficiency, and high safety [1] [2]. Traditional shaft-driven helicopters face challenges such as low flight speed, poor safety, body torque balance, and complex structure [3]. In contrast to traditional shaft-driven helicopters, tip-jet-driven helicopters generate reactive forces to rotate the rotor by high-speed jet streams at the blade tips [4]. These helicopters eliminate the need for heavy gear transmission systems

and anti-torque systems, greatly simplifying the overall structure, significantly reducing the empty weight ratio, and featuring simplicity, ease of use, and lightweight construction [5] [6]. There are two main jet methods for tip-jet rotor helicopters [7] [8] [9]: one is to install an engine at the wingtip, which generates a reaction force through the engine's jet to drive the rotor to rotate. This method has high noise, and fuel consumption, and the centrifugal force of the wingtip engine requires high strength of the rotor structure; Another way is to guide the airflow through pipelines to the rotor nozzle and spray it out, generating a reaction force to drive the rotor. Compared to directly introducing high-temperature exhaust gas into the rotor duct, introducing a gas generator can provide more gas to the rotor and better control the airflow flow and temperature.

High-concentration hydrogen peroxide is a green propellant that is easy to store, high-density, non-toxic, and non-polluting [10]. Hydrogen peroxide decomposition produces water and oxygen, which can be used as a single-component propellant or as an oxidizer [11] [12], widely used in the aerospace field [13]. There are numerous matching fuel types, such as organic amines, alcohols, hydrocarbons, and hydrazines [14]. Hydrogen peroxide/carbon-hydrogen fuel engines have advantages like being non-toxic, non-polluting, high-density specific impulse, storable, and low-cost [15]. When hydrogen peroxide serves as an oxidizer, it catalytically decomposes into high-temperature oxygen and water vapor [16], allowing the fuel to ignite and burn spontaneously in the decomposed gas without the need for a complex ignition system, making the propulsion system simple and easy to use [17].

In 1935, Germany used hydrogen peroxide as a propellant for torpedoes, missiles, and aircraft [18]. During World War II, Germany used hydrogen peroxide to drive the working fluid of the turbopump for the V-2 rocket [19]. In 1971, the UK successfully launched the "Black Arrow" launch vehicle, powered by Gamma2 and Gamma8 engines using hydrogen peroxide and kerosene as propellants. NASA's ISTAR project compared the performance of hydrogen peroxide and liquid oxygen, concluding to use of 90% hydrogen peroxide as the oxidizer for RBCC engines [20] [21]. In 2004, the United States studied a 90% hydrogen peroxide 1100 N engine thrust chamber [22]. In 2014, Poland developed a small 250 N rocket engine using 98% hydrogen peroxide/jet fuel [23].

Hydrogen peroxide is widely used in the aerospace field, and it can be used as both a single component propellant and an oxidant, making it very suitable for gas generators. By referencing rocket gas turbine combination engines, utilizing high-pressure air generated by compressors driven by engines to cool the high-temperature gases from hydrogen peroxide decomposition and the high-temperature engine exhaust, and using the mixed gas to drive the rotor, requirements such as utilizing exhaust energy (fuel-efficient), using smaller engines (weight reduction), and tip-jet control for rotor conversion (safe and flexible) can be achieved. In conclusion, this study focuses on optimizing the gas generator in a tip-jet composite power system for helicopters.

2. Thenumerical Simulation Methods

The schematic diagram of the tip-jet composite power system studied in this paper is shown in Figure 1. This composite power system comprises several components, including a piston engine, a propeller, a centrifugal compressor, a gas generator, and a tip-jet rotor. During vertical takeoff and hover, the piston engine drives the centrifugal compressor to generate compressed air, which is then introduced into the gas generator along with the high-temperature exhaust gas from the piston engine. In the gas generator, hydrogen peroxide propellant is heated by the high-temperature exhaust gas, leading to propellant decomposition and gas generation. The gases produced by propellant decomposition mix with the high-temperature exhaust gas and compressed air before entering the tip-jet rotor, where they are expelled through the rotor nozzle to generate reactionary force and drive rotor rotation. During high-speed forward flight, the piston engine drives the propeller rotation to produce forward thrust. At this point, the injection of hydrogen peroxide propellant into the gas generator is ceased, and the rotor enters autorotation.

According to the overall design scheme of the tip-jet composite power system, appropriate simplifications were made to the gas generator and tip-jet rotor sections. The overall geometric structure of the gas generator was preliminarily determined. The gas generator converges axially, with compressed air entering from inlet 1. high-temperature exhaust gas entering from inlet 2. and hydrogen peroxide propellant entering from inlet 3. The propellant rapidly decomposes at high temperature, generating gas that accelerates downstream in the gas generator along with compressed air and high-temperature exhaust gas, entering the rotor internal passage. The rotor inlet diameter is 100 mm, and the mixed gas is

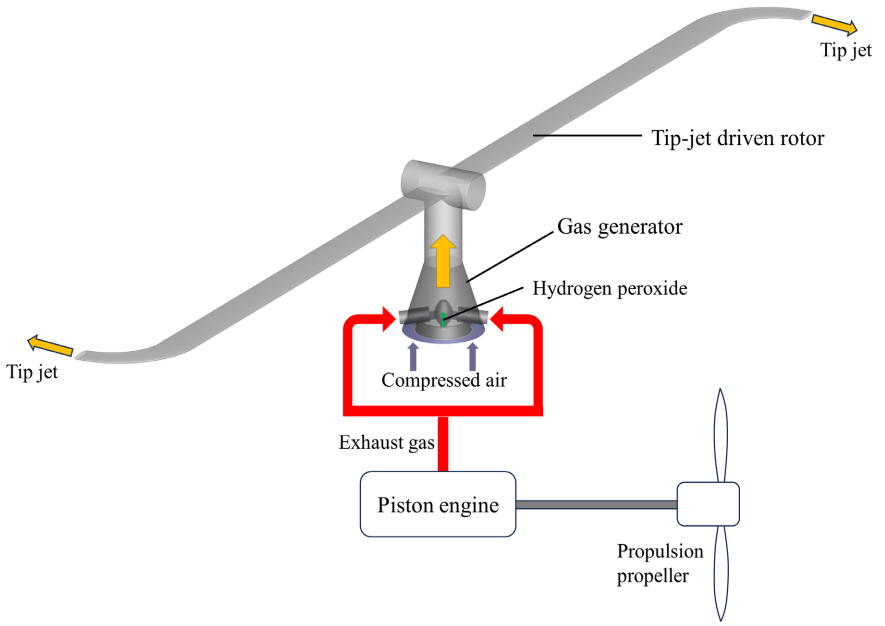

Figure 1. Schematic diagram of the tip-jet composite power system.

split from the rotor internal passage into two sides, passing through straight pipe sections and curved pipe sections before being expelled from rotor nozzles 1 and 2. The length of the single-sided straight pipe section in the rotor internal passage is 1400 mm, with a bending radius of 185 mm for the central axis in the curved pipe section and an elliptical cross-sectional shape. The cross-section of the curved pipe section in the rotor contracts, with the nozzle area being half of the straight pipe section's cross-sectional area. The long axis of the elliptical nozzle is 68 mm and the short axis is 11.3 mm. The internal area of the gas generator and the rotor internal passage was chosen as the computational domain for numerical simulation to effectively avoid errors from separately simulating the gas generator and rotor internal passage, encompassing the entire computational domain.

The three-dimensional geometric structure of the gas generator was meshed using ICEM-CFD software, employing adaptive unstructured meshes. The entire flow area of the gas generator was meshed, with important areas such as the inlet of the piston engine's high-temperature exhaust gas, the inlet of hydrogen peroxide propellant, the core mixing zone, and the rotor nozzle bend receiving mesh refinement, resulting in a total mesh count of approximately 800,000 as shown in Figure 2.

The standard k-epsilon model was used to simulate turbulent flow inside the gas generator, while the eddy dissipation model was employed to simulate the decomposition reaction of hydrogen peroxide propellant. The walls were set as adiabatic and no-slip boundaries, standard wall functions were utilized for near-wall treatment, and the SIMPLE algorithm was applied for pressure-velocity corrections. The inlet for compressed air used a pressure inlet with a total pressure of 0.13 MPa and a total temperature of 320 K, while the inlet for high-temperature exhaust gas from the piston engine was a mass flow inlet with a mass flow rate of 0.035 kg/s and a total temperature of 900 K (initially assumed as 900 K due to heat dissipation from the exhaust of the piston engine to the gas generator). The

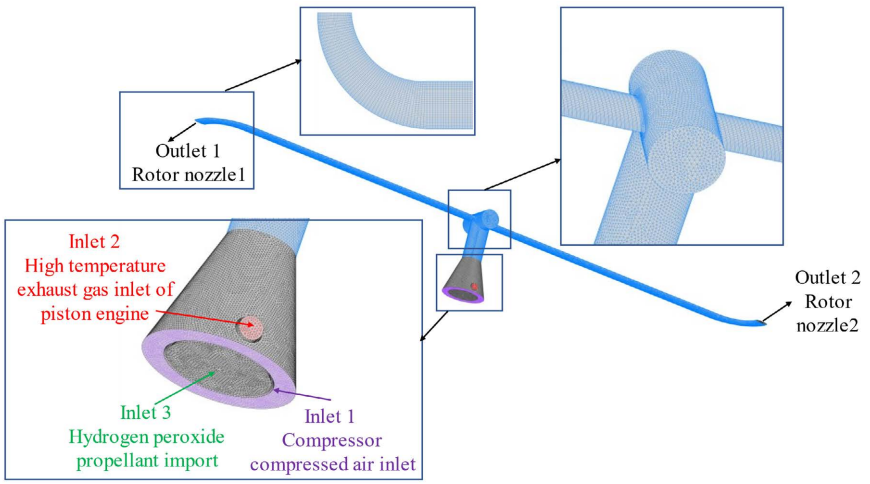

Figure 2. Schematic diagram of the computational domain grid.

hydrogen peroxide propellant was a 70% industrial solution, simulated by adding it as a discrete phase, with a mass flow rate of 0.007 kg/s for liquid hydrogen peroxide and 0.003 kg/s for liquid water, both at a total temperature of 288 K. Based on previous calculations, when 0.01 kg/s of hydrogen peroxide was added at 0.2 MPa, the nozzle velocity was 40 m/s, so the discrete phase nozzle velocity was set at 40 m/s. The exit pressure of the rotor nozzle was 101325 Pa, and the rotor speed was 50 rad/s.

3. Results of the Gas Generator Optimization

3.1. Analysis of Flow Field Characteristics of the Gas Generator

The center section and exit temperature contours of the gas generator are shown in Figure 3. Due to the relatively small mass flow rate of hydrogen peroxide and the majority of the decomposition heat being converted into the latent heat of vaporization of liquid water and liquid hydrogen peroxide, the high-temperature region inside the gas generator is primarily above the hydrogen peroxide propellant nozzle, where it is exposed to the high-temperature exhaust gas from the engine. The maximum temperature reaches 876 K, as the high-temperature exhaust gas drives the flow of liquid hydrogen peroxide and liquid water, with the heat mostly absorbed by the liquid droplets, accelerating their evaporation and resulting in lower temperatures below the hydrogen peroxide nozzle.

The center section and exit velocity contours of the gas generator are shown in Figure 4. From the figures, it can be observed that the high-temperature exhaust gas from the engine rapidly enters the gas generator and encounters the hydrogen peroxide solution outside the propellant nozzle. The hydrogen peroxide quickly decomposes at high temperatures, simultaneously consuming heat during the transition from liquid to gas. Due to the high velocity of the exhaust gas, it carries the reacting hydrogen peroxide downward, resulting in a high-speed streak in the velocity contour moving downwards. Subsequently, it flows towards the gas generator exit along with the compressed air inlet until the velocity becomes relatively uniform at the exit of the gas generator. As the gas generator is in a converging nozzle state, the exit velocity increases.

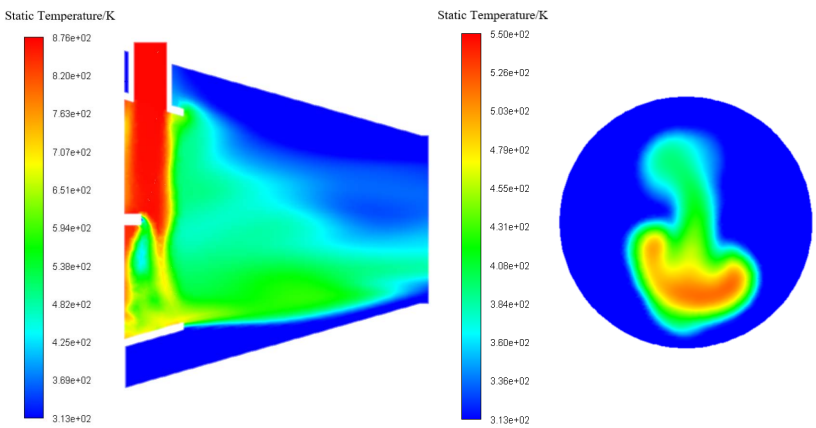

Figure 3. The center section and exit temperature contours of the gas generator.

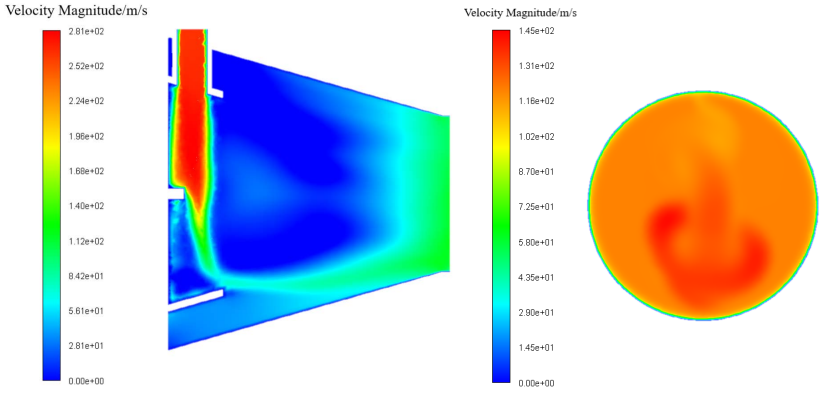

Figure 4. The center section and exit velocity contours of the gas generator.

From the contour of the flow field above, it is evident that the fluid distribution at the outlet of the gas generator is not uniform and lacks symmetry. This asymmetry is further exacerbated upon entering the rotor inner channel, resulting in systematic asymmetry on the two rotors and leading to a series of issues. There is significant room for optimization in the intake of high-temperature exhaust gas and the internal structure of the gas generator. Additionally, the impact of propellant components and injection amount on the gas generator and the tip-jet composite power system is crucial.

3.2. The Influence of the High-Temperature Exhaust Gas Intake Mode and the Addition of the Inner Cavity

To address the systematic asymmetry, the most direct approach is to change the single inlet of high-temperature exhaust gas to a dual inlet. Based on the dual inlet design for high-temperature exhaust gas, two cases were set up: case 1 and case 2. In case 1, the inlet of high-temperature exhaust gas is perpendicular to the flow axis of the gas generator, while in case 2, the inlet of high-temperature exhaust gas is angled with respect to the flow axis of the gas generator. Both cases have a grid size of approximately 1.4 million cells. The compressed air inlet uses a pressure inlet with a total pressure of 0.15 MPa and a total temperature of 320 K. The high-temperature exhaust gas inlet uses a mass flow inlet with a mass flow rate of 0.03 kg/s and a total temperature of 900 K. The propellant hydrogen peroxide has a mass flow rate of 0.01 kg/s and a total temperature of 473 K (initially assumed at 473 K due to heating in the pipeline before the nozzle). Other conditions are the same as in the previous case studies.

The temperature contour at the center cross-section of the gas generator under different methods of high-temperature exhaust gas intake is shown in **Figure 5**. It can be observed from the figure that in the case of the vertical exhaust gas inlet, the high-temperature region has a larger impact on the outlet of the gas generator compared to the case with the angled exhaust gas inlet. The outlet temperature of the gas generator with the angled exhaust gas inlet is more uniform, with smaller temperature differentials, which is favorable for the flow field in the rotor inner channel. In both cases, the high-temperature zone generated

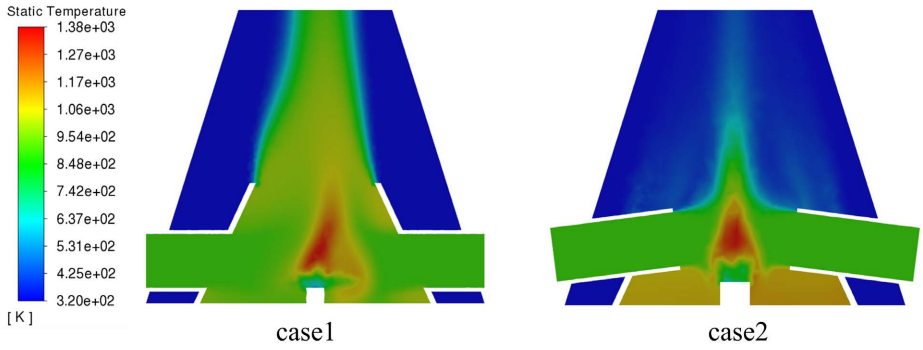

Figure 5. Temperature contour of the central section of the gas generator under different intake methods of high-temperature exhaust gas.

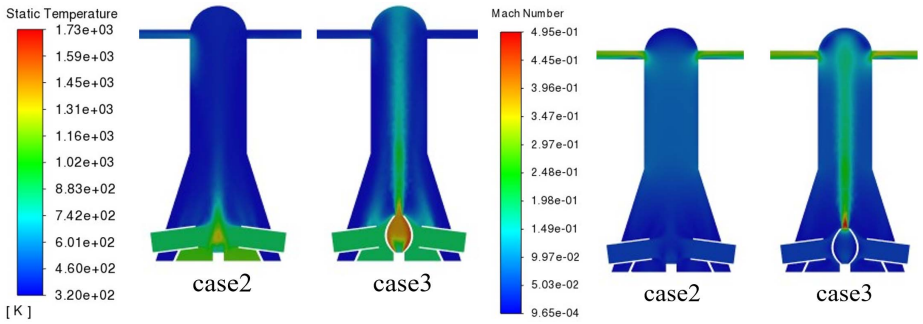

Figure 6. Contours of temperature and velocity at the center section of a gas generator with or without an inner cavity.

by the decomposition reaction of the propellant in the gas generator is concentrated at the central part of the gas generator, reaching temperatures exceeding 1300 K. Clearly, at this temperature, more reliable structural solutions need to be considered, such as the possibility of setting up an internal cavity structure behind the propellant nozzle, similar to a combustion chamber in an aircraft engine, to confine the reaction to a relatively high-pressure area.

Building on case 2, case 3 introduces an internal cavity in the gas generator behind the propellant nozzle, while keeping all other initial boundary conditions the same as in case 2. Figure 6 illustrates the temperature and velocity contour of the central cross-section flow field of the gas generator with and without the internal cavity. From the figure, it can be observed that the propellant reacts completely within the internal cavity, with the high-temperature region located inside the gas generator's cavity. The velocity at the outlet of the cavity is significantly higher compared to the case without an internal cavity. These flow field characteristics can have a noticeable impact on the inlet of the rotor, ultimately affecting the magnitude of the available moment in the composite power system.

The section parameters of the above examples are filled in Table 1.

The comparison of data from the table indicates that the method of high-temperature exhaust gas inlet and the presence of an internal cavity in the gas generator have an impact on the available moment in the composite power

Table 1. Aerodynamic parameters of composite power systems with different gas generator structures.

Aerodynamic parameters	Case 1	Case 2	Case 3
Compressed air inlet mass flow rate (kg/s)	0.255	0.246	0.244
Rotor nozzle total pressure (MPa)	0.121	0.121	0.121
Rotor nozzle total temperature (K)	418.12	435.43	437.33
Rotor nozzle absolute velocity/(m/s)	203.77	204.25	203.01
Rotor nozzle mass flow rate (kg/s)	0.295	0.286	0.284
Available moment (N·m)	92.37	89.59	88.27

system. The calculation results for the available moment show that the maximum is for the vertical inlet, followed by the slanted inlet, and the slanted inlet with an internal cavity being the lowest. A slanted inlet is more favorable for airflow distribution compared to a vertical inlet. The available moment is slightly larger without an internal cavity than with one, suggesting that there is significant room for optimization in the internal cavity structure, which could be further explored in future research.

3.3. The Influence of Propellant Components and Injection Amount

In order to analyze the effect of propellant components and injection amount on the characteristics of this composite power system, numerical simulations were conducted for case 3 with 0.01 kg/s of hydrogen peroxide, case 4 with 0.03 kg/s of hydrogen peroxide, and case 5 with 0.008 kg/s of hydrogen peroxide and 0.002 kg/s of kerosene. Other conditions remained consistent with the previous calculation examples.

The temperature distribution at the center section of the gas generator and rotor nozzle was compared, as shown in **Figure 7**. The high-temperature exhaust gas (900 K) from the engine enters the gas generator diagonally, enveloping the internal cavity of the gas generator. Prior to the nozzle, there is a short section of duct for the propellant, with a temperature of 473 K at the propellant nozzle. Once the propellant enters the internal cavity of the gas generator surrounded by high-temperature exhaust gas, it further decomposes and reacts exothermically, leading to an increase in temperature. The temperature contour of the gas generator's center section shows that the temperature inside the cavity is higher, with the internal cavity temperature of case 5 significantly higher than that of case 3, due to the decomposition of hydrogen peroxide and combustion of kerosene, resulting in high-temperature gas being sprayed from the cavity. The gas temperature at the compressed air inlet is relatively lower and, enveloped by the high-temperature gas, mixes with the gas sprayed from the internal cavity of the gas generator, cooling the high-temperature gas. The impact of high-temperature gas can be seen mainly in the vicinity of the gas generator's central axis, extending to the rotor center. The temperature contour of the rotor nozzle shows that the elliptical nozzle has higher temperatures near the major axis end and relatively lower temperatures in the central region. The temperature distribution of the nozzle is not uniform, primarily due to the increased

viscous friction at the major axis of the nozzle, resulting in average temperatures of 437.33 K, 605.03 K, and 855.68 K for the rotor nozzle cross-sections of cases 3, 4, and 5, respectively. In conclusion, the composition and injection rate of propellant directly affect the temperature field inside the gas generator, thereby influencing the temperature of the rotor nozzle.

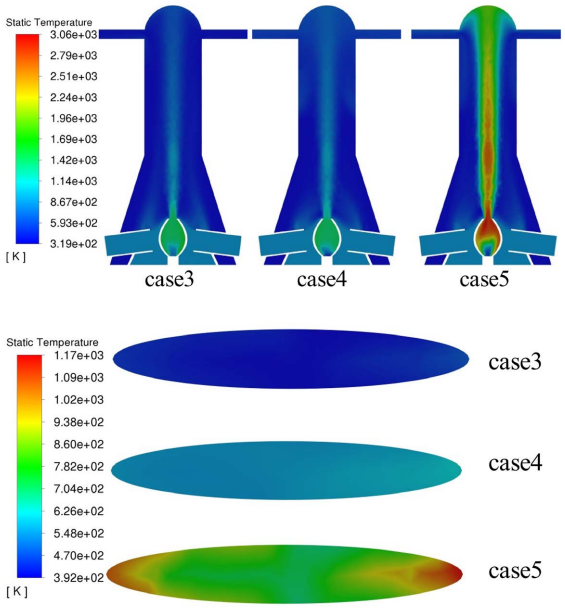

Figure 7. The gas generator center section and rotor nozzle temperature contours.

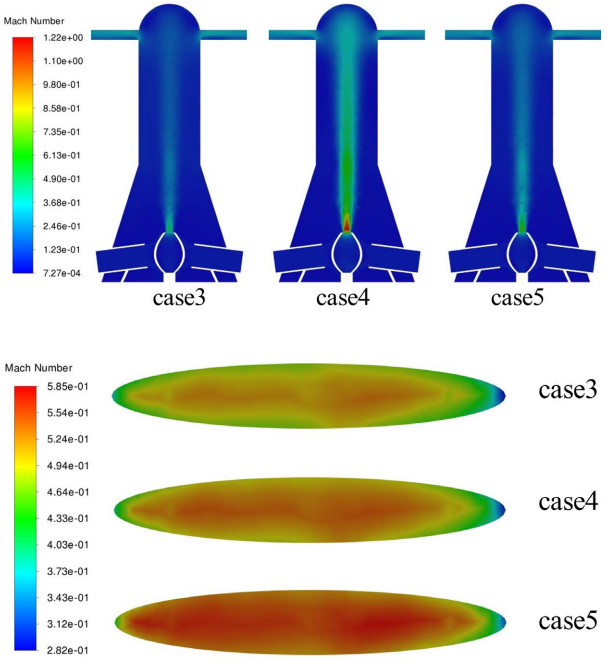

Figure 8. The gas generator center section and rotor nozzle velocity contours

Table 2. Aerodynamic parameters of composite power systems with different propellant components and injection amount.

Aerodynamic parameters	Case 3	Case 4	Case 5
Theoretical reaction heat of propellant	28.84	86.52	114.27
Compressed air inlet mass flow rate (kg/s)	0.244	0.174	0.159
Rotor nozzle total pressure (MPa)	0.121	0.122	0.124
Rotor nozzle total temperature (K)	437.33	605.03	855.68
Rotor nozzle absolute velocity/(m/s)	203.01	249.39	304.68
Rotor nozzle mass flow rate (kg/s)	0.284	0.234	0.199
Available moment (N·m)	88.27	89.58	93.03

The velocity contour of the center section of the gas generator and the rotor nozzle are shown in Figure 8. The exit velocity of the gas generator's internal cavity is the highest in the entire flow field, and it subsequently mixes with compressed air and high-temperature exhaust gas, leading to a reduction in velocity. The influence of different propellant components and injection amount on the flow field velocity persists until the rotor nozzle. The area of the rotor nozzle is smaller than the internal channel cross-section, and the fluid is expelled after passing through the final convergent bend, resulting in an increase in the absolute velocity at the nozzle exit. The exit velocity of the nozzle is relatively uniform, with only a slight decrease in velocity near the major axis end of the elliptical nozzle.

Under the same rotational angular velocity (50 rad/s) conditions, the analysis and comparison of temperature and velocity distributions at the center section of the gas generator and the rotor nozzle reveal that different propellants have a significant impact on the aerodynamic characteristics of the composite power system. The aerodynamic parameter data for different propellant components and injection amount at various cross-sections of the composite power system are presented in Table 2.

The formula for calculating the available moment is given by:

$$M = q_m \cdot v_a \cdot L \tag{1}$$

where M represents the available moment, q_m represents the mass flow rate of the rotor nozzle, V_a represents the absolute velocity of the rotor nozzle, and L represents the length of the rotor.

Based on the data above, the characteristics of the rotor nozzle in the composite power system can be obtained, as shown in Figure 9. Cases 1, 2, and 3 represent scenarios where the gas generator structure is altered, while cases 3, 4, and 5 represent scenarios where the propellant for the gas generator is modified.

In cases where the gas generator structure is altered, Figure 9(a) indicates that the available moment decreases as the mass flow rate of the rotor nozzle de-

creases, Figure 9(c) shows that the change in available moment is not significantly related to the absolute velocity of the rotor nozzle, and Figure 9(e) reveals that the available moment decreases as the temperature of the rotor nozzle increases. This is because changes in the gas generator structure alter the internal pressure distribution, directly affecting the mass flow rate of compressed air and the rotor nozzle mass flow rate. According to the formula for calculating available moment (Equation 1), when the absolute velocity and length of the rotor nozzle remain constant, a decrease in the rotor nozzle mass flow rate results in a reduction in available moment. Additionally, as the mass flow rate of compressed air at low temperatures decreases, the temperature of the rotor nozzle increases. Lowering the temperature of the rotor nozzle is one of the goals of optimizing the gas generator structure, as it helps reduce heat dissipation losses and increase available moment.

In cases where the propellant is modified, Figure 9(b) shows that the available moment increases as the mass flow rate of the rotor nozzle decreases, Figure 9(d) indicates that the available moment increases with the increase in the absolute velocity of the rotor nozzle, and Figure 9(f) demonstrates that the available moment increases as the temperature of the rotor nozzle rises. This is because different propellants alter the total energy of the system, with total energy reflected in internal energy (temperature) and kinetic energy (mass flow rate and velocity). The theoretical heat of reaction of propellants in cases 3, 4, and 5 increases successively, leading to an increase in released heat, resulting in an increase in internal pressure in the gas generator, an increase in the absolute velocity and temperature of the rotor nozzle, but also causing a decrease in the mass flow rate of compressed air at low temperatures, leading to a decrease in the mass flow rate of the rotor nozzle and a further increase in the temperature of the rotor nozzle. According to the formula for calculating available moment (Equation 1), when the length of the rotor remains constant, an increase in the absolute velocity of the rotor nozzle results in an increase in available moment, but a decrease in the mass flow rate of the rotor nozzle leads to a decrease in available moment. Ultimately, the incremental increase in available moment in cases 3, 4, and 5 compared to the increase in theoretical heat of reaction of the propellants is relatively small, with a sharp rise in the temperature of the rotor nozzle indicating an increase in heat dissipation losses. While enhancing the energy of the propellant is beneficial for increasing available moment, the selection of propellants should also consider factors such as pressure, temperature, and heat dissipation losses in the gas generator. Lowering the temperature of the rotor nozzle, increasing the absolute velocity and mass flow rate of the rotor nozzle, is advantageous for reducing heat dissipation losses and increasing available moment. Studying the impact of propellant components and injection amount on the aerodynamic characteristics of the composite power system can help select more suitable propellants for the system, leading to further optimization in the future.

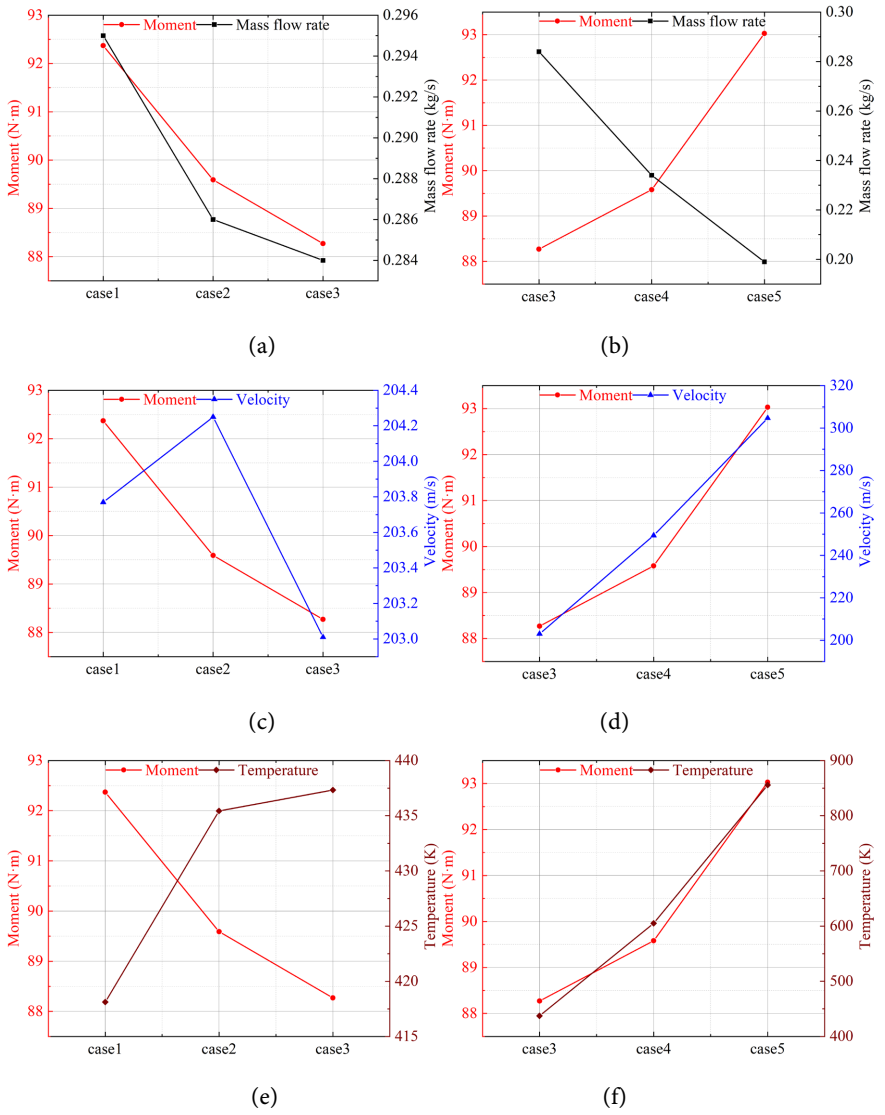

Figure 9. Characteristics of the rotor nozzle in the composite power system.

4. Conclusions

This paper presents numerical simulations of the channels within a composite power system under different gas generator structures and various propellant components and injection amounts, leading to the following conclusions:

1) In the case of a vertical high temperature exhaust gas inlet, the impact of high-temperature regions on the gas generator outlet is more significant than in the case of a slanted high temperature exhaust gas inlet. The gas generator outlet temperature is more uniform with a slanted high temperature exhaust gas inlet, resulting in smaller temperature differentials, which is advantageous for the flow field within the rotor inner channel.

2) The high-temperature regions generated by the propellant decomposition reaction are concentrated in the central part of the gas generator. By introducing an internal cavity structure similar to a flame tube at this location, the reaction

occurs in a relatively stable high-temperature zone. Simulation results demonstrate that the internal cavity significantly improves the temperature and velocity distribution within the gas generator's internal flow field, ultimately impacting the magnitude of the available moment in the composite power system. There is ample room for further optimization of the internal cavity structure, which warrants additional in-depth research.

3) Increasing the energy of the propellant is beneficial for enhancing the available moment. However, simply raising the theoretical heat of the reaction of the propellant may not necessarily lead to a significant increase in the available moment and could potentially result in substantial heat dissipation losses. The selection of propellants should consider factors such as pressure, temperature, and heat dissipation losses within the gas generator. This conclusion is consistent with the conclusion in references [24] [25] [26], which states that it is not advisable to increase the jet reaction force solely by increasing the gas temperature inside the rotor duct. This not only fails to increase the jet reaction moment, but also poses issues with the material's high-temperature resistance.

In future work, it is possible to expand the research on the influence of gas generator structure and gas generator inlet parameters on the aerodynamic characteristics of the system, providing a reference for the design of tip-jet rotor composite power systems.

Acknowledgements

This work is supported by the National Nature and Science Foundation of China under Grant No. 52166003, Nanchang Hangkong University Graduate Innovation Special Fund (YC2022070).

Conflicts of Interest

The authors declare no conflicts of interest regarding the publication of this paper.

References

[1] Wu, X.M. and Mou, X.W. (2021) A Perspective of the Future Development of Key Helicopter Technologies. *Acta Aerodynamica Sinica*, **39**, 1-10. https://doi.org/doi:10.7638/kqdlxxb-2021.0042

[2] Liu, Z.Y. and Cheng, X.G. (2020) The Research of Process and Future Development of High-Speed Helicopter. *Proceedings of the 9th Youth Science and Technology Forum of the Chinese Aeronautical Society*, Shaanxi, China, 17-19 November 2020, 89-99.

[3] Jiang, Y., Zhang, B. and Huang, T. (2015) CFD Study of an Annular-Ducted Fan Lift System for VTOL Aircraft. *Aerospace*, **2**, 555-580. https://doi.org/10.3390/aerospace2040555

[4] Chen, J., Li, L., Huang, G. and Xiang, X. (2018) Numerical Investigations of Ducted Fan Aerodynamic Performance with Tip-Jet. *Aerospace Science and Technology*, **78**, 510-521. https://doi.org/10.1016/j.ast.2018.05.016

[5] Leishman, J.G. (2004) Development of the Autogiro: A Technical Perspective.

Journal of Aircraft, **41**, 765-781. https://doi.org/10.2514/1.1205

[6] Mitchell, C. and Vogel, B. (2003) The Canard Rotor Wing (CRW) Aircraft—A New Way to Fly. *Proceedings of the AIAA International Air & Space Symposium & Exposition*: *The Next* 100 *Years*, Dayton, 14-17 July 2003, Article 2517. https://doi.org/10.2514/6.2003-2517

[7] Li, Y.B., Ma, D.L. and Niu, L.Y. (2011) Power-Matching Methodology in Tip-Jet Drive Rotor Design. *Journal of Aerospace Power*, **26**, 1787-1793. https://doi.org/10.13224/j.cnki.jasp.2011.08.020

[8] Head, R. (1992) Reaction Drive Rotors-Lessons Learned (Hero Had a Good Idea-But). *Guidance*, *Navigation and Control Conference*, Hilton Head Island, 10-12 August 1992, Article 4279. https://doi.org/10.2514/6.1992-4279

[9] Rutherford, J.W., Bass, S.M. and Larsen, S.D. (1993) Canard Rotor/Wing: A Revolutionary High-Speed Rotorcraft Concept. *Aerospace Design Conference*, Irvine, 16-19 February 1993, Article 1175. https://doi.org/10.2514/6.1993-1175

[10] Li, Q., Nie, S., Liu, Y.K., Pan, L. and Ma, M.Y. (2011) Numerical Simulation of Combustion Characteristics for Thrust Chamber in Hydrogen Peroxide/Kerosene Engine. *Journal of Rocket Propulsion*, **37**, 35-39. https://doi.org/10.3969/j.issn.1672-9374.2011.04.006

[11] Nosseir, A.E.S., Cervone, A. and Pasini, A. (2021) Review of State-of-the-Art Green Monopropellants: For Propulsion Systems Analysts and Designers. *Aerospace*, **8**, Article 20. https://doi.org/10.3390/aerospace8010020

[12] Paravan, C., Hashish, A. and Santolini, V. (2023) Test Activities on Hybrid Rocket Engines: Combustion Analyses and Green Storable Oxidizers—A Short Review. *Aerospace*, **10**, Article 572. https://doi.org/10.3390/aerospace10070572

[13] Okninski, A., Surmacz, P., Bartkowiak, B., Mayer, T., Sobczak, K., Pakosz, M., Kaniewski, D., Matyszewski, J., Rarata, G. and Wolanski, P. (2021) Development of Green Storable Hybrid Rocket Propulsion Technology Using 98% Hydrogen Peroxide as Oxidizer. *Aerospace*, **8**, Article 234. https://doi.org/10.3390/aerospace8090234

[14] He, F., Fang, T., Li, Y.Y. and Mi, Z.T. (2006) Development of Green Liquid Propellants. *Chinese Journal of Explosives & Propellants*, **29**, 54-57. https://doi.org/10.3969/j.issn.1007-7812.2006.04.015

[15] Lin, G., Ling, Q.C. and Li, F.Y. (2005) A Study of Thrust Chamber Technology Using Hydrogen Peroxide. *Journal of Rocket Propulsion*, **31**, 1-4. https://doi.org/10.3969/j.issn.1672-9374.2005.03.001

[16] Parzybut, A., Surmacz, P. and Gut, Z. (2023) Impact of Hydrogen Peroxide Concentration on Manganese Oxide and Platinum Catalyst Bed Performance. *Aerospace*, **10**, Article 556. https://doi.org/10.3390/aerospace10060556

[17] Liu, J.H. (2007) Research on Dynamic Characteristics of Hydrogen Peroxide Engine. Ph.D. Thesis, National University of Defense Technology, Changsha.

[18] Wernimont, E., Ventura, M., Garboden, G. and Mullens, P. (1999) Past and Present Uses of Rocket Grade Hydrogen Peroxide. General Kinetics, Aliso Viejo.

[19] Ventura, M., Wernimont, E. and Dillard, J. (2007) Hydrogen Peroxide-Optimal for Turbomachinery and Power Applications. 43*rd AIAA*/*ASME*/*SAE*/*ASEE Joint Propulsion Conference & Exhibit*, Cincinnati, 8-11 July 2007. https://doi.org/10.2514/6.2007-5537

[20] Quinn, J. (2002) Oxidizer Selection for the ISTAR Program (Liquid Oxygen versus Hydrogen Peroxide). 38*th AIAA*/*ASME*/*SAE*/*ASEE Joint Propulsion Conference &*

Exhibit, Indianapolis, 7-10 July 2002. https://doi.org/10.2514/6.2002-4206

[21] Quinn, J. (2003) ISTAR: Project Status and Ground Test Engine Design. 39*th AIAA/ASME/SAE/ASEE Joint Propulsion Conference and Exhibit*, Huntsville, 20-23 July 2003.https://doi.org/10.2514/6.2003-5235

[22] Wernimont, E. and Durant, D. (2004) Development of a 250 Lbfv Kerosene-90% Hydrogen Peroxide Thruster. 40*th AIAA/ASME/SAE/ASEE Joint Propulsion Conference and Exhibit*, Fort Lauderdale, 11-14 July 2004. https://doi.org/10.2514/6.2004-4148

[23] Okninski, A., Bartkowiak, B., Sobczak, K., Kublik, D., Surmacz, P., Rarata, G., Marciniak, B. and Wolanski, P. (2014) Development of a Small Green Bipropellant Rocket Engine Using Hydrogen Peroxide as Oxidizer. 50*th AIAA/ASME/SAE/ASEE Joint Propulsion Conference*, Cleveland, 28-30 July 2014. https://doi.org/10.2514/6.2014-3592

[24] Li, B.B. (2015) Study on the Aerodynamic Characteristics of the Pressure Jet Rotor. Master's Thesis, Nanjing University of Aeronautics and Astronautics, Nanjing.

[25] Elmahmodi, A., and Algattus, S. (2012) Analysis of Different Propulsion Systems for Tip Jet Rotor System. *Journal of Engineering Research*, **15**, 47-54.

[26] Pandya, S. and Aftosmis, M. (2001) Computation of External Aerodynamics for a Canard Rotor/Wing Aircraft. 39*th AIAA Aerospace Sciences Meeting and Exhibit*, Reno, 8-11 January 2001. https://doi.org/10.2514/6.2001-997